ACS MEASUREMENT SCIENCE Au
AN OPEN ACCESS JOURNAL OF THE AMERICAN CHEMICAL SOCIETY

pubs.acs.org/measureau

Article

Development of Multiplexed Bead-Based Immunoassays for Profiling Soluble Cytokines and CD163 Using Mass Cytometry

Jieyi Liu, Bedilu Allo,* and Mitchell A. Winnik*

Cite This: *ACS Meas. Sci. Au* 2022, 2, 629–640

Read Online

ACCESS | Metrics & More | Article Recommendations | Supporting Information

ABSTRACT: Bead-based immunoassays are multiparametric analysis allowing for the simultaneous quantification of a large number of biomarkers within a single sample. Mass cytometry is an emerging cytometric technique that offers a high multiplexing capacity in a high-throughput setting but has not yet been applied to bead-based assays. In this study, we developed a multiplex bead-based immunoassay of cytokines and CD163 designed for mass cytometry (MC). A set of 11 types of lanthanide-encoded microbeads were synthesized by two-stage dispersion polymerization as classifier candidates for the assay. These beads were then decorated with different Abs on the surface to capture the target cytokines in solution. Gold nanoparticles were employed as reporters to identify the binding of target cytokines on the classifier surface. As a proof-of-concept study, we first developed four-plex and nine-plex assays of mixtures of cytokines in standard solutions. The MC signal intensities of these immunoassays were responsive to the concentration differences in the standard solutions with high detection sensitivities at low analyte concentrations. Finally, we examined a sample of peripheral blood mononuclear cells (PBMCs) with the nine-plex assay, comparing an unstimulated sample with a sample stimulated to promote cytokine secretion.

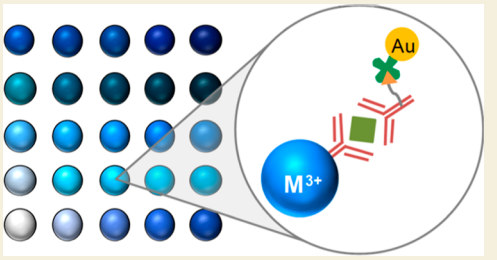

KEYWORDS: *mass cytometry, bead-based assay, immunoassay, cytokine, chemokine*

INTRODUCTION

Cytokines are soluble signaling protein molecules produced by cells at picomolar to nanomolar concentrations to regulate immune responses and modulate cellular activities. They are an exceptionally large and diverse group of pro- and anti-inflammatory factors in the body.[1] Immune dysregulation can lead to excessive cytokine release with devastating consequences, a phenomenon referred to as a cytokine storm. An early example, referred to as cytokine release syndrome, accompanied infusion of an anti-CD3 antibody.[2] An event that had a larger impact on the medical community was the cytokine storm that developed after chimeric antigen receptor (CAR) T-cell therapy reported in 2010.[3] This report was cited by two prominent reviews of the state of development of assays for cytokine levels in blood and serum as well as assays that monitored factors that promoted cellular release of cytokines.[4,5] A variety of disorders have been described as causes of cytokine storm such as sepsis, hemophagocytic lymphohistiocytosis, autoinflammatory disorders, and, most recently, coronavirus disease 2019 (COVID-19).[6,7]

A number of studies have examined the nature of cytokine profiles accompanying severe COVID-19 infection and noted, for example, markedly higher levels of IL-2R, IL-6, IL-10, and TNF-α.[8,9] Elevated levels of IL-6 have been shown to have predictive value in identifying patients who will need mechanical ventilation in COVID-19.[10] Review articles summarize these findings but point out that there are some inconsistencies in cytokine and chemokine levels detected in different patients.[6,11,12] There are limitations to current research tools to fully investigate the mechanism of cytokine generation and action.

A number of different techniques are used to detect cytokine and chemokine levels in blood, in serum, and in cell studies. Enzyme-linked immunosorbent assays (ELISAs) are the most extensively used Ab-based immunoassays to analyze individual cytokines in biological samples. However, ELISA assays require substantial amounts of sample and are time consuming when large numbers of cytokines are analyzed at once.[13,14] Bead-based immunoassays are a technology platform that offers information-rich multiparametric analysis in a high-throughput setting. Bead-based assays employing fluorescent dyes for signal detection are the current gold standard for multiplexed cytokine analysis, and kits for cytokine analysis are commercially available. In this type of assay, polymer microbeads are labeled with two or three different fluorescent dyes at different concentrations to well-defined intensities.

Received: June 18, 2022
Revised: August 24, 2022
Accepted: August 24, 2022
Published: October 6, 2022

https://doi.org/10.1021/acsmeasuresciau.2c00038
ACS Meas. Sci. Au 2022, 2, 629–640

Successful antigen detection is recognized by a reporter antibody (Ab) labeled with dye with a distinct emission.[15−21] A recent report from the College of American Pathologists describes results of a proficiency-testing program in which well-defined samples of four cytokines (IL-1, IL-6, IL-8, and TNF-α) at three levels of concentration were analyzed by multiple techniques in six different laboratories. These surveys administered from 2015 to 2018 reveal significant variability in cytokine analysis between laboratories and variability across method, even within the same laboratory.[22] This study highlights some of the current challenges in quantitative cytokine detection.

Mass cytometry (MC) is an emerging analytical technique that combines the features of flow cytometry and elemental mass spectrometry to simultaneously analyze the signals of isotopic labels on microbead samples.[23] MC can accurately detect and quantify different metal isotopes with minimal channel spillovers and background noise due to the low abundance of heavy metal isotopes in biological samples.[24] Compared with fluorescence-based bead assays, MC offers an opportunity to characterize sample features with enhanced resolution and sensitivity.[25] MC has been used as a multiplexed format for cytokine detection. O'Gorman et al. used 16 Abs labeled with metal-chelating polymers as part of a broader assay of cell surface markers and signaling proteins in a single-cell system-level analysis of human Toll-like receptor activation.[26] A similar approach from the Nolan group was taken in a study of brain myeloid cells in mouse neuro-inflammation.[27]

From this perspective, we have set out to develop a multiplexed bead-based assay designed for MC. In this type of assay, the classifier beads are labeled with heavy metal isotopes, in principle at different levels of metal incorporation. Each classifier bead carries a different Ab on its surface. The reporter can be a metal or metal oxide nanoparticle (NP) with an appropriate Ab of other biorecognition element bound to its surface. Samples are injected stochastically into the plasma torch of an inductively coupled plasma time of flight mass spectrometer. The instrument is capable of single mass resolution over the range from m/z 89 (Y) to m/z 209 (Bi).[28] Thus, in principle, a very high level of multiplexing is possible.

$$n = K^M - 1 \quad (1)$$

For example, the theoretical maximum variability (n) in a bead-based MC assay is given by eq 1, where K refers to the levels of metal concentration in the microbeads (including zero) and M is the number of different isotopes encoded in the beads. The term -1 accounts for beads with zero metal content for all of the isotopes, which cannot be detected.[29] The isotopes of 15 lanthanide elements encompass 36 detection channels. We have shown that we can label the beads with three different levels of lanthanide content with baseline resolution.[30] For this example, with $K = 4$ and $M = 36$, a very large variety of multiplexing ($n \sim 10^{21}$) can theoretically be created.

In this first report of a bead-based immunoassay by MC, we set out to test a proof of concept using cytokine analysis as our target. In these first attempts, we examined some of the strengths and shortcomings of this approach. Our intention is to establish a baseline set of data that can be used as the starting point for further optimization of this technique.

We began with a four-plex analysis of a mixture of four cytokines. Based upon optimization of this analysis, we extended our study to a nine-plex assay in which we uncovered some challenges associated with non-specific binding of the reporter NPs. Finally, we examined the nine-plex assay with a sample of peripheral blood mononuclear cells (PBMCs), comparing an unstimulated sample with a sample stimulated to promote cytokine secretion.

EXPERIMENTAL SECTION

Materials

The synthesis and characterization of metal-encoded microbeads employed in this study are reported in the Supporting Information. Buffers and RPMI 1640 cell culture medium used in this study were purchased from ThermoFisher. Phorbol 12-myristate 13-acetate (PMA) and ionomycin for stimulation were received from Millipore-Sigma. Antibodies (Abs), biotinylated Abs, and cytokine standards were purchased from Biolegend and R&D Systems (see Table S1 in the Supporting Information). Streptavidin-conjugated gold nanoparticles (AuNPs, 10 nm, 10 OD) were bought from Abcam. Cryopreserved human peripheral blood mononuclear cells (PBMCs) were purchased from Immunospot (CTL, LP-188 HHU20130715). Nanogold-Streptavidin (Nanoprobe), EQFour Element Calibration Beads (EQ4), and Cell-ID Pd Barcoding Kits were kindly provided by Fluidigm Canada (now Standard BioTools Canada).

Preparation of a Set of Metal-Encoded Classifier Beads

To develop bead-based assays in MC, we first need to prepare a library of microbeads labeled with various metal ions that can be individually identified by MC. In our previous publication, we described a method of encoding microbeads with controlled levels of metal ions by introducing polymerizable metal complexes of the structure M(DTPA-VBAm$_2$) in two-stage dispersion polymerization (DisP) reactions. In this study, we prepared a panel of 11 binary-metal-encoded 3 μm polystyrene (PS) microbeads employing this novel method. The details of microbead synthesis are described in the Supporting Information.

To prepare classifier beads that can capture the target analytes in immunoassays, each type of the metal-encoded beads was surface modified with one type of Ab specific for a cytokine by a proprietary method developed at Fluidigm Canada (now Standard BioTools Canada). Each type of classifier bead used in this study was prepared in a single batch to eliminate the effect of batch-to-batch variation.

Stimulation of PBMCs for Cytokine Secretion

Cryopreserved human peripheral blood mononuclear cells (PBMCs) were thawed and added to a pre-warmed RPMI serum-free medium (10 mL) containing 0.5 mL of CTL anti-aggregate wash supplement 20× (CTL-AA-001). The PBMCs in the sample were spun down by centrifugation (8 min, 300 rpm). The supernatant was aspirated after centrifugation. The PBMCs were then resuspended with a warm serum-containing complete RPMI (10 mL). An aliquot of this PBMC suspension in RPMI (4.8 mL, 4.8 × 10^6 cells) was transferred to a PS tube and stimulated with a PBS solution (100 μL) containing phorbol myristate acetate (PMA, 25 nmol) and ionomycin (100 nmol). The sample with stimulants was incubated for 5 h at 37 °C with 5% CO_2. The simulated PBMC suspension was then centrifuged to settle the cells. The supernatant was collected as the stimulated sample and stored at −80 °C prior to bead-based assays. Another aliquot of the PBMC suspension in RPMI media was treated under the same conditions in parallel except for the addition of stimulants (PBS only). The unstimulated sample was collected as a control in this experiment.

Optimization of Bead-Based Sandwich Immunoassay Protocol for MC

To optimize the assay protocol, several multiplexed bead-based assays were carried out using serial dilutions of recombinant proteins of

https://doi.org/10.1021/acsmeasuresciau.2c00038
ACS Meas. Sci. Au 2022, 2, 629−640

Scheme 1. Schematic Diagram for the Multiplexed Bead-Based Sandwich Immunoassays by MC Carried out in a 96-Well Filter Plate[a]

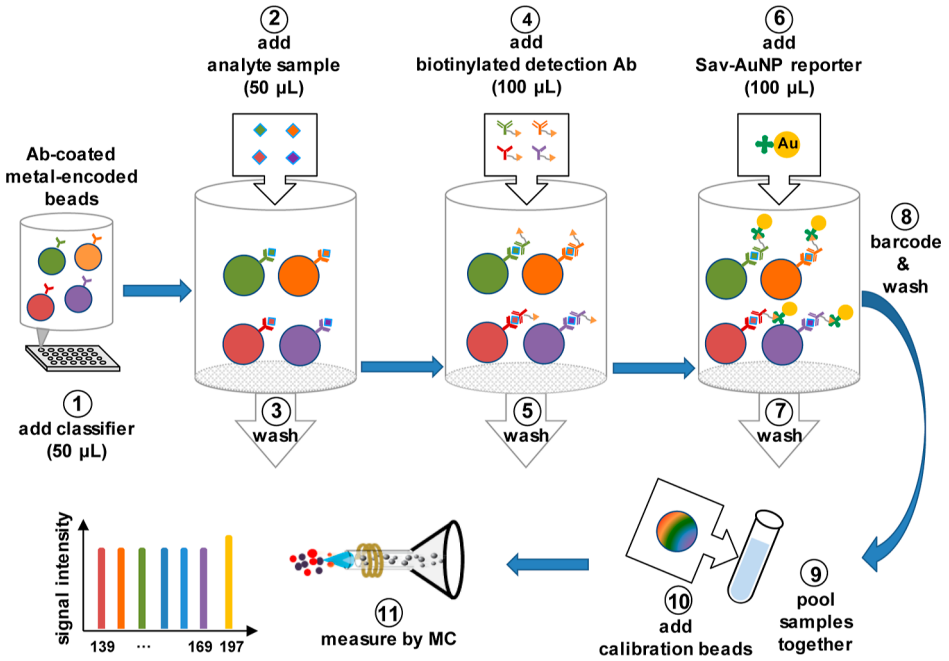

[a]Metal-encoded microbeads were surface modified with capture Abs and employed as the classifier to recognize the target analytes in samples. The detailed protocol is described in the Experimental Section.

cytokine and chemokine standard samples. The assayed samples were analyzed by MC to plot standard curves and assess assay parameters. Scheme 1 shows the assay procedure developed in this study.

A series of four-plex assays were carried out to analyze IL-4, IL-6, TNFα, and IFNγ in a 10-point standard curve. In these experiments, four types of capture Ab-coated metal-encoded classifier microbeads were first mixed in approximately equal numbers in PBS-based assay diluent (0.5% BSA in PBS). The classifier bead dispersion was then transferred to 10 wells of a 96-well filter plate (filter cutoff: 0.45 μm). Each well contained ca. 2 million beads in the dispersion (50 μL), and each well represented a single analyte concentration point of the standard sample. A series of 10 standard solutions (50 μL each) consisting of four analytes at four-fold serial dilutions from 0 to 20,000 pg/mL analyte concentration were added to each well, respectively. The mixture of standard solution and classifier beads in each well was first gently mixed with a pipette and then incubated on a rotary microplate shaker (1200 rpm for 30 s and then 900 rpm for 2 h) at room temperature. After the incubation, the well content was aspirated using a manual multiscreen vacuum manifold system. The classifier beads with analytes captured on their surface were washed by two redispersion−aspiration cycles with homemade washing buffer (200 μL, 0.025% TWEEN 20 in PBS) to remove possible uncaptured analytes. Once the washing buffer was removed from the well by vacuum filtration, a detection Ab cocktail (100 μL, 0.5% BSA in PBS) containing 2.5 μg/mL of four types of biotinylated Abs [anti-IL-4 (MP4-25D2), anti-IL-6 (MQ2-39C3), anti-TNFα (MAb11), and anti-IFNγ (4S.B3)] was transferred to each well. The classifier beads were redispersed with detection Abs by pipette agitation. The mixture of classifier beads and detection Abs was incubated at room temperature for 1 h on a microplate shaker (900 rpm). After incubation, the mixture was filtered and washed by two redispersion−filtration cycles with washing buffer to remove unbound detection Abs on the classifier beads. The classifier beads on the filter were then redispersed with a dispersion (100 μL) of streptavidin-conjugated gold nanoparticles (AuNPs) as the reporter. The reporter dispersion was prepared by diluting the AuNP dispersion 1:200 from the vendor with 0.5% BSA buffer. The mixture of classifier beads and AuNP reporter was incubated on a shaker (900 rpm) for 1 h and washed by two filtration−redispersion cycles with washing solution and two cycles with PBS buffer (100 μL). In order to measure multiple assays in a single MC run, the assay sample (100 μL) in each well was incubated with Fluidigm's (now Standard BioTools) palladium-based barcoding reagent (40 μL, 3× dilution of a stock solution in Cell-ID Pd Barcoding Kit). The barcoding staining reaction was incubated for 30 min with agitation and quenched by two filtration−redispersion cycles with 0.5% BSA solution (200 μL) and two cycles with water (100 μL). A total of 10 barcoded assay samples were combined in one test tube and examined by MC employing EQ4 beads as a calibration standard. Typically, 2×10^5 to 3×10^5 bead events per test tube were collected by MC. On average, approximately 1000−1500 bead events were counted per classifier.

In a typical multiplex assay of a sample with unknown analyte concentrations, different types of metal-encoded classifier beads that can capture the target analytes were first mixed in equal numbers in an assay diluent and then transferred to a 96-well filter plate. In each well, the classifier bead dispersion (50 μL) can analyze one unknown sample by adding an aliquot (50 μL) of the sample solution to the well. The mixture was then incubated, washed, and stained with detection Abs and AuNP reporter in a similar procedure as that described in the abovementioned assays of standard samples.

Instrumentation

Mass Cytometry. The bead-based barcoded assay products were analyzed by mass cytometry (Helios, a CyTOF system, Fluidigm (now Standard BioTools)). In a typical MC sample acquisition, barcoded immunoassay samples and EQ4 beads as an internal standard were pooled into a test tube and introduced to the MC system at a speed of 30 μL/min. After acquisition, the MC signals were normalized using signals from the EQ4 beads and debarcoded to separate the results from each sample. To analyze the MC result of one assay sample, the singlets of all the classifier beads included in the assay were first identified and gated on the ^{140}Ce−^{142}Ce dot plot. Each type of classifier beads was then gated based on their signature signals of metal encoding. The median signal intensities of the reporter, ^{197}Au for AuNPs, were reported as the results.

https://doi.org/10.1021/acsmeasuresciau.2c00038
ACS Meas. Sci. Au 2022, 2, 629−640

Table 1. Summary of the Particle Size, Median Intensities of MC Signals, and Target Analytes of Classifier Microbeads Prepared by Two-Stage DisP of Styrene with M(DTPA-VBAm$_2$) Metal Complexes

microbead	bead size[a]		MC median signal intensities[b] (counts per bead)						target
ID	d (μm)	CV (%)	^{139}La	^{140}Ce	^{141}Pr	^{159}Tb	^{165}Ho	^{169}Tm	analytes[c]
C-1	3.0	1	1060	1100	1120	1130	1180	1110	IL-18
C-2	2.8	1	862	881					TNFα
C-3	2.9	1		857	871				IL-6
C-4	3.0	1		1050		1130			IFNγ
C-5	2.9	1		791			979		IL-4
C-6	2.9	1		874				984	CD163
C-7	2.9	1	900	937		1170			CXCL-9
C-8	2.9	1		815	864	960			IL-10
C-9	2.8	1		844		935	958		IL-1β
C-10	2.8	1		778		963		947	[d]
C-11	2.8	1		768			898	898	[d]

[a]The mean diameter (d) and the coefficient of variation (CV) of microbead samples were evaluated by measuring the diameters of at least 300 microbeads in their SEM images. [b]The median signal intensities of microbeads were measured by MC using EQ4 beads as a calibration standard. The robust coefficient of variation (RCV) of the signal intensities for each type of these microbeads was in the range of 7−9% (not shown in the table). [c]To capture the target analytes in assay samples, capture Abs were covalently coupled to the surface of microbeads by a proprietary bead-surface functionalization and biomolecule coupling method developed at Fluidigm Canada (now Standard BioTools Canada). [d]No target analyte was assigned to the microbeads in this study. The microbeads can be surface modified with bioaffinity reagents for the capture of analytes.

RESULTS AND DISCUSSION

The objective of this study is to develop multiplexed bead-based sandwich immunoassays for detection of soluble proteins in biological fluids using MC. In our experimental design, we employ metal-encoded microbeads as the solid support for an immunoassay and gold (Au) NPs as the reporter. The capture Ab of each immunoassay is covalently coupled to one of the microbead sets, each of which comprises microbeads with a uniform, distinct content of heavy metal isotopes. Once coupled with capture Abs, microbeads from different sets as classifiers can be pooled together for the multiplexed assays and separated later after data acquisition. Data are acquired on a MC and analyzed by FlowJo software (see Scheme 1 for the experimental design). The immunoassay results in a variable ^{197}Au signal intensity of the Au NP reporter, proportional to the amount of analyte bound to the surface of each microbead. Since MC quantifies the content of different heavy metal isotopes in each microbead, the pool of microbeads can be separated into individual bead set with the median ^{197}Au signal intensity of NP reporter for each bead set. Due to this feature, many assays can be carried out simultaneously, allowing for the multiplexed quantification of multiple analytes in a single measurement. In addition, the concentration of the analytes in the sample can be determined by extrapolation from an internal standard.

Syntheses of Metal-Encoded Classifier Beads by Dispersion Polymerization

Initially, we envisioned the synthesis of 32 types ($2^5 = 32$) of classifier microbeads binary encoded by varying the incorporation of five types of lanthanide metal ions (La^{3+}, Pr^{3+}, Tb^{3+}, Ho^{3+}, and Tm^{3+}) with intensity levels of either 0 or ca. 1000 (±20%) counts per bead. In addition, Ce^{3+} ions would be incorporated into each of the beads at a similar level. The cerium isotopes ^{140}Ce and ^{142}Ce can serve as a microbead identifier for the convenience of gating classifier signals in the MC results. As a demonstration of the design strategy, a set of 11 binary-metal-encoded 3 μm polystyrene (PS) microbeads for bead-based assays were synthesized by a series of two-stage dispersion polymerization (DisP) by following the bead synthesis protocol reported in our previous publications.[30]

Key details of the bead synthesis and characterization are described in the Supporting Information. A scanning electron microscopy image of the bead sample C-1 (see Table S2 and S3 for synthesis details) is presented in panel (a) of Figure S1 in the Supporting Information. It shows that these microbeads are uniform with a mean diameter of 3.0 μm and a CV of 1%. The median intensity levels of MC signals of the encoded isotopes were in the range of 1000−1200 counts per bead. Panel (b) of Figure S1 shows a similar level of incorporation efficiencies among six metals in the bead synthesis. Table 1 provides a summary of the beads that we prepared, their mean diameters (and CV values) as well as the labeling pattern and signal intensities in MC detection. We note that these 11 types of microbeads are uniform (CV ~1%) and share a similar size with mean diameters in the range of 2.8−3.0 μm. For antibody attachment, the beads were coated via a proprietary technology developed at Fluidigm (now Standard BioTools), and the Abs attached to the respective classifier beads are listed in Table 1.

In addition, the metal ions incorporated in these microbeads generated MC signals at a similar intensity level of 800−1200 counts per bead. Since all the microbeads (C1 to C11) carried Ce^{3+} that produced Ce signals at a similar level in MC, we were able to analyze a mixture of all the beads in a single MC measurement and isolated the singlets of 11 types of microbeads in one gating from the ^{140}Ce−^{142}Ce dot plot (see Figure 1a). The dot plots in Figure 1b−k demonstrate the gating strategy to individually identify each type of classifier microbeads based on their signature signals of metal encodings. Because the microbeads in this set of classifier beads are uniform with MC signal intensities at similar levels, a gating template was created in FlowJo software based on this microbead gating strategy to simplify the data analysis process of multiplex assays.

Initial Optimization of Bead-Based Sandwich Immunoassay Conditions

Initial optimization of assay protocols for bead-based sandwich immunoassay for MC application was carried out by measuring the cytokine levels in a series of solutions with known

https://doi.org/10.1021/acsmeasuresciau.2c00038
ACS Meas. Sci. Au 2022, 2, 629−640

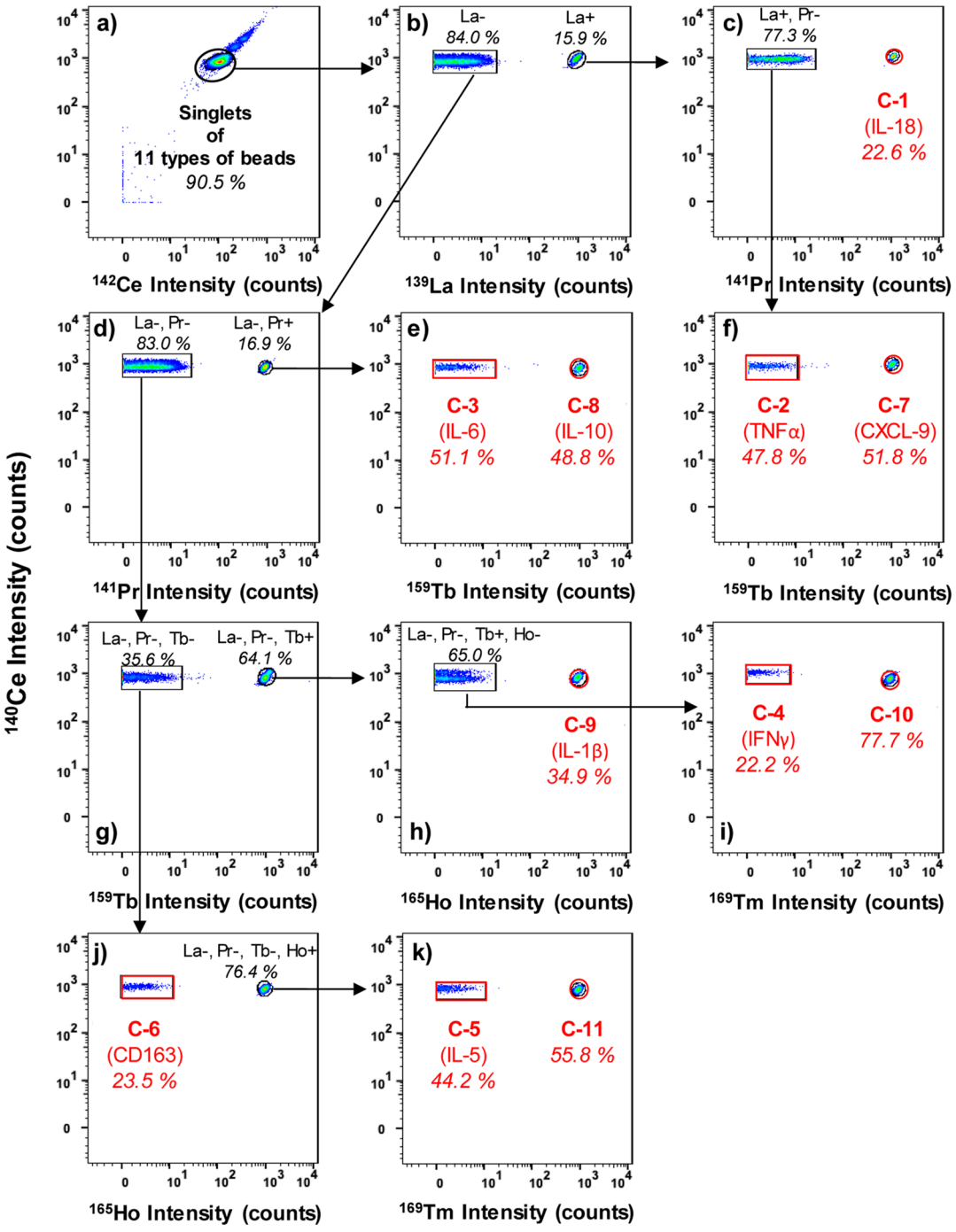

Figure 1. (a) ^{140}Ce−^{142}Ce isotopic dot-plot diagram of a mixture of 11 types of classifier microbeads (C-1 to C-11). The oval circle isolates the singlet events of 11 types of microbeads. (b−k) Dot-plot diagrams showing the gating strategies to individually identify C-1 to C-11 microbeads by MC.

concentrations of cytokine standard solutions. The effects of different assay reagents and conditions on the assay results were evaluated by examining the standard curves from these measurements. In the first stage of the assay development, we used a series of four-plex assays of standard solutions to test the candidate reporters, which are commercially available streptavidin-conjugated nano-sized Au reporters, and optimized the reporter concentration in the assays. We then extended our assays to nine-plex assays to investigate the effect of detection Ab concentration on the assay performance.

In a typical experiment, we prepared a series of solutions containing known concentrations of target cytokines by diluting the standard solutions with 0.5%BSA-buffer (0.5% BSA in PBS). Each of these standard solutions (50 μL) was mixed with a cocktail of Ab-modified classifier beads (50 μL) in a filter plate. During the incubation, the Ab-modified classifier beads in the assay can capture their target analytes in the sample. After 1 h of incubation, these classifier beads were washed by filtration to remove the unbound molecules in the sample. A cocktail of biotinylated detection Abs (100 μL) was then added to the assay, followed by redispersing the classifier

https://doi.org/10.1021/acsmeasuresciau.2c00038
ACS Meas. Sci. Au 2022, 2, 629−640

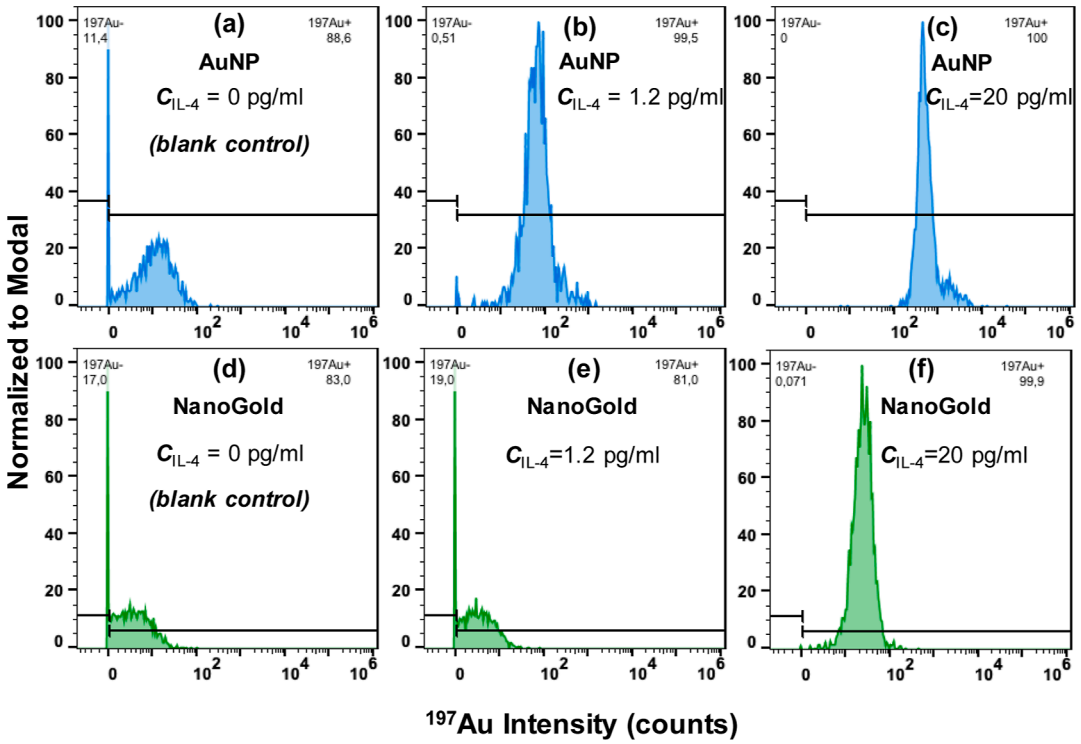

Figure 2. Histograms of the reporter signal intensities on IL-4 classifier beads (C-5) in a series of four-plex assays of standard solutions at various IL-4 concentrations. (a–c) AuNP was employed as the reporter in four-plex assays of standard solutions containing IL-4 at concentrations of 0, 1.2, and 20 pg/mL, respectively. (d–f) NanoGold was employed as the reporter in four-plex assays of standard solutions containing IL-4 at 0, 1.2, and 20 pg/mL, respectively.

beads. In this step, the biotinylated Abs in the cocktail can recognize the analyte molecules captured on the classifier bead surface. These classifier beads in the assay were then washed on the filter to eliminate unbound detection Abs. Next, a streptavidin-conjugated Au mass tag dispersion (100 μL) was applied to the assay as a reporter. These mass tags attach to the biotinylated detection Abs on the classifier beads by the streptavidin–biotin interaction.[31] After washing off the unattached reporter particles, the assay sample was examined by MC for the metal content in the individual microbead event. The principles of this bead-based sandwich immunoassay design are illustrated in Scheme 1.

After signal acquisition, we analyzed the assay results in FlowJo software through their dot-plot diagram. Figure 1 demonstrates the gating strategy employed in our study. The singlet events of all classifier beads were first isolated in the panel (a) of Figure 1. Each classifier bead in the gated singlet events was then individually identified through a series of gating steps in the dot-plot diagrams shown in the panel (b–k) of Figure 1. The ^{197}Au signal in each classifier event was then examined and reported as the assay signal.

Selection of Reporter. To find a proper metal-labeled mass tag to report the analyte binding on classifier beads, we examined two types of commercially available streptavidin-conjugated reporters, small diameter gold clusters (NanoGold, $d \approx 1.4$ nm) and somewhat larger diameter gold nanoparticles (AuNP, $d \approx 10$ nm). We estimate that each AuNP with a diameter of 10 nm contains 31,000 Au atoms, while each NanoGold with a diameter of 1.4 nm only contains 85 Au atoms assuming both of these gold mass tags share a density of 19.3 g/cm^3. Thus, a AuNP tag can potentially generate a much brighter signal in MC than a NanoGold tag, if these Au tags are ionized similarly in the ICP torch. These mass tags were tested as reporters in a series of four-plex assays analyzing standard solutions consisting of four analytes at 12 concentrations.

The histograms shown in Figure 2 demonstrate the signal intensities of reporters on IL-4-classifier beads in the four-plex assays. AuNP was employed as the reporter in the assays shown in Figure 2a–c. A few positive ^{197}Au signals were recorded in Figure 2a when IL-4 was absent in the blank control solution. The median value of all the events in this plot was reported as a background noise control to reflect the nonspecific binding of reporter NPs to the classifier beads. The intensity peaks of ^{197}Au signals on the IL-4-classifier beads were shifted upfield in the panel (b,c) of Figure 2, as the IL-4 concentration in the assays increased from 1.2 to 20 pg/mL. At 1.2 pg/mL, some events with the ^{197}Au signal intensity at nearly 0 count per bead were recorded in Figure 2b. These "0" events could be instrument noise due to artifacts during the signal acquisition process or due to some classifier beads carrying small numbers of reporters that were below the MC detection limit. To eliminate the uncertainties and simplify the data analysis process, the median intensity values of the positive events (reporter signal intensity >1 count per bead) in the positive samples are reported and plotted in this study.

In the histograms shown in panels (d–f) of Figure 2, NanoGold was employed as the reporter to analyze standard solutions containing IL-4 at concentrations of 0, 1.2, and 20 pg/mL, respectively. Much weaker intensities of the NanoGold reporter signals for ^{197}Au on the IL-4-classifier beads were observed, compared with the results of assays using AuNPs as the reporter, presumably because each NanoGold reporter contains much less Au ions than each AuNP does. More events

https://doi.org/10.1021/acsmeasuresciau.2c00038
ACS Meas. Sci. Au 2022, 2, 629–640

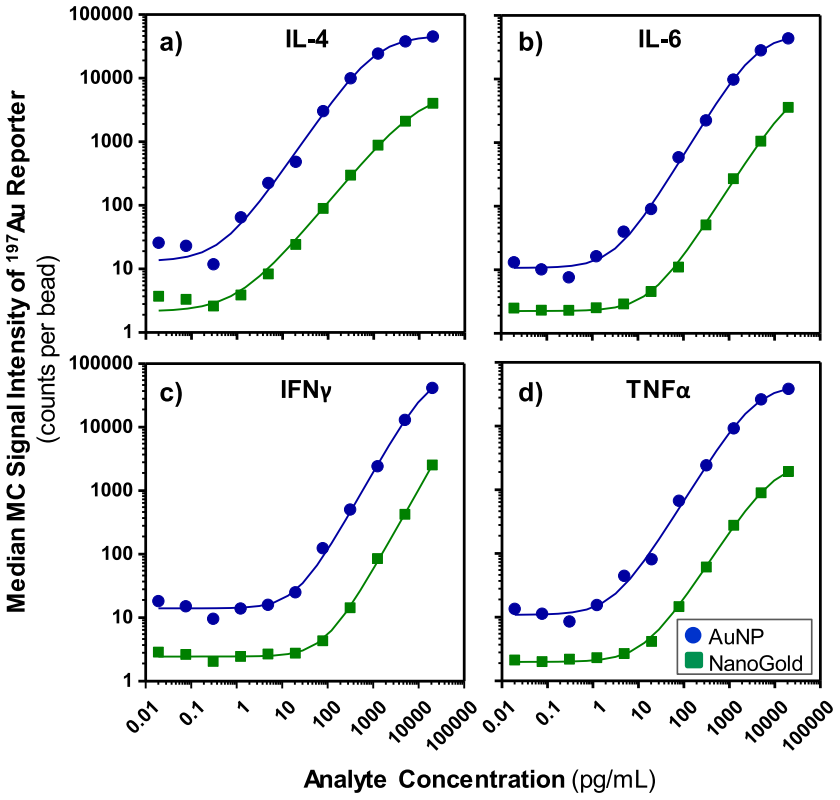

Figure 3. Standard curves of two sets of four-plex assays for (a) IL-4, (b) IL-6, (c) IFNγ, and (d) TNFα. The x-axis in each plot represents the analyte concentration, and the y-axis represents the median MC signal intensity of NPs attached to the corresponding classifier beads. Two different types of streptavidin-conjugated reporter (AuNP and NanoGold) were investigated in these four-plex assays. The results are presented for the AuNP as blue-filled circles (●) and for the NanoGold as green filled squares (■). Negative events with ^{197}Au signal intensities of ≤1 count per bead were excluded from the statistical analysis for median intensities. The dose−response curves were drawn by fitting the experimental results with a four-parameter logistic regression model.

with signal intensities of ∼0 are shown in the panel (e) histograms compared with panel (b) of Figure 2.

A typical dose-responsive standard curve of a bead-based assay starts with a low and flat region when the analyte concentration is low. The curve then rises with the increase of the analyte concentration, followed by a plateau at a higher concentration.[18,20,32] In this study, the detection range of an assay was estimated based on the slope region of the standard curve. Within this slope region, analyte concentration is presumably measurable.

Figure 3 summarizes the median MC signal intensities of different types of NPs attached to classifier beads at different analyte concentrations. In the low concentration region (up to ca. 1 pg/mL), the signal intensities of both types of reporters are low (*ca.* 10 counts per bead) and insensitive to the increase of the analyte concentration. The signal detected for the third concentration (0.31 pg/mL) was slightly lower than that detected for the adjacent concentrations. We have no explanation for this result. At higher analyte concentrations ranging from 1 to 1000 pg/mL, the signal intensities of these reporters increase significantly with the increase of the analyte concentration. The signal intensities of AuNPs approach a plateau when the concentrations of analytes are above 1000 pg/mL, while the curves of assays using NanoGold as the reporter show similar trends but much lower intensities compared with that using AuNP as the reporter. Because of the much higher signal intensities obtained at lower analyte concentrations in these assays, AuNPs were chosen as the reporter candidate for the subsequent bead-based assays in this study to optimize the lower limit of detection.

Optimization of the Reporter Concentration. We then investigated the effect of reporter NP concentration on assay signal intensity levels. In this study, the stock AuNP dispersion was diluted 200, 400, and 800 times with 0.5% BSA buffer. These dilutions were then employed as reporter solutions in three sets of four-plex assays to analyze standard solutions. Figure S2 shows the standard curves of the four-plex assays carried out under different AuNP concentrations. The signal intensities of AuNP at all three dilutions showed minimal differences at analyte concentrations above 20 pg/mL. The detection limits of assays stained with 200× diluted AuNP dispersion were as low as 0.3 pg/mL for IL-4, IL-6, and TNFα, while that for IFNγ was slightly higher at 1.2 pg/mL. 200× AuNP dilution was selected as the optimal condition for the bead-based assays in the following studies.

Optimization of Detection Ab Concentration (in Nine-Plex Assays). After using a series of four-plex assays as a proof-of-concept experiment, we then tried to expand the multiplexing capacity of the assays to nine analytes by adding the analysis of IL-1β, IL-10, IL-18, CD163, and CXCL-9 to the panel. We adapted the experimental conditions developed in the four-plex assays to analyze a series of standard solutions containing nine analytes. In the first set of nine-plex assays, the concentration of each type of biotinylated Ab in the detection Ab cocktail was 2.5 μg/mL. The results are plotted as blue-filled circles (●) in Figure 4. We noticed that the median intensity levels of AuNP signals on all types of classifier beads

https://doi.org/10.1021/acsmeasuresciau.2c00038
ACS Meas. Sci. Au 2022, 2, 629−640

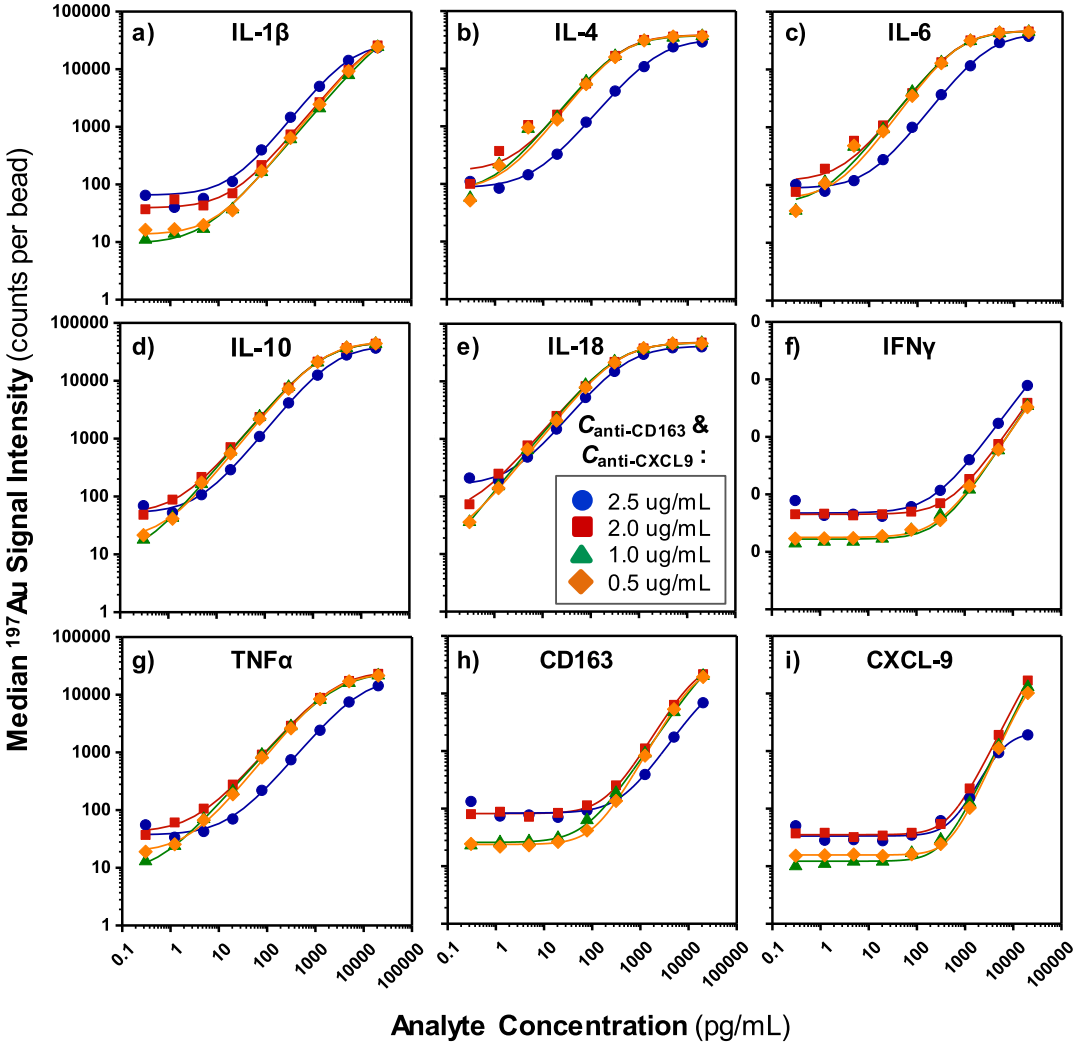

Figure 4. Standard curves of four sets of nine-plex assays for (a) IL-1β, (b) IL-4, (c) IL-6, (d) IL-10, (e) IL-18, (f) IFNγ (g) TNFα, (h) CD163, and (i) CXCL-9. The x-axis in each plot represents the analyte concentration. The y-axis in each plot represents the median MC signal intensity of AuNP attached to the corresponding type of classifier beads. To minimize the background noise at low analyte concentrations, the concentrations of biotinylated anti-CD163 and anti-CXCL9 in the detection Ab cocktails were reduced from 2.5 to 2.0, 1.0, and 0.5 μg/mL, while the concentrations of other detection Abs were kept constant at 2.5 μg/mL in the cocktails. The results of these assays are plotted for anti-CD163 and anti-CXCL9 Ab concentrations of 2.5 μg/mL with filled circles (●), of 2.0 μg/mL with filled squares (■), of 1.0 μg/mL with filled triangles (▲), and of 0.5 μg/mL with filled diamonds (◆). Negative events with ^{197}Au signal intensities of ≤1 count per bead were excluded from the statistical analysis for median intensities. The dose−response curves were drawn by fitting the experimental results with a four-parameter logistic regression model.

at low analyte concentrations (≤1.22 pg/mL) were relatively high (∼100 counts per bead) and not sensitive to the concentration changes. Compared with the previous four-plex assays, these nine-plex assays were less sensitive to detect analytes at low analyte concentrations. These relatively high levels of signal intensities at low analyte concentrations were attributed to background noise in the assays, possibly a consequence of non-specific binding.

To trace the source of the high background noise in nine-plex assays, we first scaled back the assays and carried out a set of seven-plex assays to analyze IL-1β, IL-4, IL-6, IL-10, IL-18, IFNγ, and TNFα in standard samples in the absence of CD163 and CXCL-9. The classifier beads for CD163 and CXCL-9 (C-6 and C-7) were also not added in these seven-plex assays. We opted to omit the detection of CD163 and CXCL-9 in these seven-plex assays, in part because the detection Abs for CXCL-9 are polyclonal, and that may lead to more non-specific binding. In addition, the cross-reactivity and interference of anti-CD163 Abs with interleukins (ILs) are unclear. In these seven-plex assays, the concentrations of detection Abs remained at 2.5 μg/mL. The results of these seven-plex assays are plotted in Figure S3 as filled circles (●). The standard curves of IL-4, IL-6, IL-10, and IL-18 assays start to increase with the increase in corresponding analyte concentrations from as low as ≥0.3 pg/mL, indicating low detection limits for these assays. Overall, the detection of all seven analytes in these seven-plex assays was fairly sensitive at low analyte concentrations. We also measured the background noise of the seven-plex assays by analyzing a blank sample. Since biotinylated anti-CD163 and anti-CXCL-9 were absent from the detection Ab cocktail, the results of this control experiment are shown as red columns in Figure S4 and annotated as "0 μg/mL". The background noise in these control assays was so weak (<1 count per bead) that the red columns in the figure

https://doi.org/10.1021/acsmeasuresciau.2c00038
ACS Meas. Sci. Au 2022, 2, 629−640

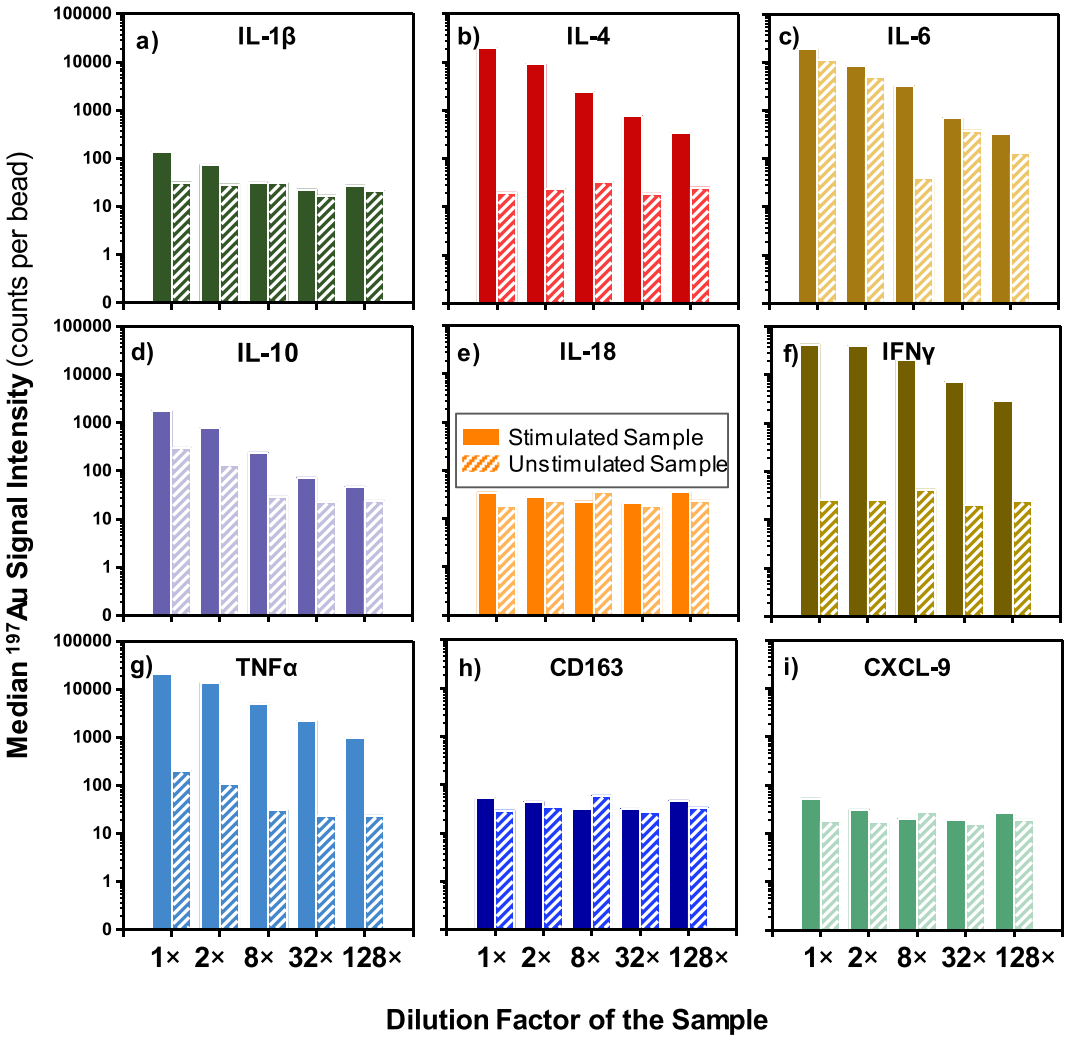

Figure 5. Median ^{197}Au signal intensities of AuNP reporter attached to classifier beads in nine-plex assays for the analysis of (a) IL-1β, (b) IL-4, (c) IL-6, (d) IL-10, (e) IL-18, (f) IFNγ, (g) TNFα, (h) CD163, and (i) CXCL-9 in the stimulated and unstimulated PBMC samples at different sample dilution ratios. To measure the extracellular cytokine release by PBMCs, the stimulated and unstimulated samples were collected from the supernatants of the PBMC suspensions in culture media with/without PMA/ionomycin stimulation. Solid columns in the figure represent the assay results of the stimulated samples, while striped columns represent the assay results of the unstimulated samples. In a typical assay, sample solution (50 μL) without dilution or diluted at the ratios of 2×, 8×, 32×, or 128× was added to the classifier dispersion (50 μL). The detection Ab concentrations of anti-CD163 and anti-CXCL9 in the assays were 0.5 and 1.0 μg/mL, while the concentration of other detection Abs was 2.5 μg/mL.

are almost invisible, suggesting the low non-specific binding in these seven-plex assays.

We then introduced CD163 and CXCL-9 separately into two sets of eight-plex assays, denoted as "7 + CD163" and "7 + CXCL-9" in Figure S3, to individually examine the possible interaction of anti-CD163 or anti-CXCL9 to the detection of other analytes. The concentration of detection Abs used in the eight-plex assays was 2.5 μg/mL for each of the eight detection Abs. The data shown as squares (■) and triangles (▲) in Figure S3 are the standard curves of these two types of eight-plex assays. We noted that the median signal intensities of these eight-plex assays of standard solutions with low analyte concentrations (≤1.22 pg/mL) were slightly higher than those of the seven-plex assays. Overall, these seven-plex and eight-plex assays show much higher sensitivity with low analyte concentrations and lower background noise, compared with that of the nine-plex assays described in Figure 4 as filled circles (●). This phenomenon suggests that the high level of background noise we observed in the nine-plex assays is likely due to the non-specific binding of biotinylated anti-CD163 and anti-CXCL-9 to the classifier beads.

To minimize the non-specific binding in the nine-plex assays, we carried out three sets of nine-plex assays, in which the concentrations of biotinylated anti-CD163 and anti-CXCL-9 were reduced to 2.0, 1.0, and 0.5 μg/mL, while the concentrations of other detection Abs remained at 2.5 μg/mL in the detection Ab cocktail. We opted to lower the concentrations of the detection anti-CD163 and anti-CXCL-9 in these assays to reduce the non-specific binding. The standard curves of these nine-plex assays are plotted in Figure 4. For the assays of the standard solutions containing low concentrations (≤1.22 pg/mL) of the analytes, the median signal intensities in the assays that employed low concentrations (0.5 and 1.0 μg/mL) of biotinylated anti-CD163 and anti-CXCL-9 Abs are significantly lower than those obtained by employing higher concentrations (2.0 and 2.5 μg/mL) of

https://doi.org/10.1021/acsmeasuresciau.2c00038
ACS Meas. Sci. Au 2022, 2, 629−640

detection Abs. In the assays of the standard solutions with high analyte concentrations (≥1250 pg/mL), the signal intensity levels and assay sensitivities are similar under all of the experimental conditions. Overall, the detection sensitivities at low analyte concentrations and detection ranges for the analytes were improved, when the concentrations of biotinylated anti-CD163 and anti-CXCL-9 Abs in the detection Ab cocktails were lowered to 0.5 and 1.0 μg/mL. As shown in Figure S4, the background noises in these nine-plex assays of blank solutions are also substantially reduced as the concentrations of biotinylated anti-CD163 and anti-CXCL-9 Abs decreased from 2.0 to 0.5 μg/mL. Based on these results, it seems that the non-specific binding of biotinylated anti-CD163 and anti-CXCL-9 to classifier beads can be minimized by reducing their detection Ab concentrations in the assays. Some other optimization of the incubation parameters (i.e,. block reagent) may also help to reduce the non-specific binding as a direction for future work.[33]

Bead-Based Sandwich Immunoassays of Cytokines in Biological Samples

As a proof-of-principle experiment, to examine the performance of the nine-plex assay on biological samples, we purchased a commercial uncharacterized PBMC sample (CTL-UP1), stimulated in cell culture media (RPMI) supplemented with PMA/ionomycin, and analyzed the extracellular release of cytokines in the supernatant of the stimulated PBMC suspension by the nine-plex assays using our optimized assay conditions. PMA has a structure analogous to diacylglycerol and can diffuse through the cell membrane into the cytoplasm. In the cytoplasm, PMA activates protein kinase C. When used in combination with ionomycin, a calcium ionophore that triggers calcium release, a moderate level of cytokine is released from cells. An unstimulated sample was collected from the supernatant of an unstimulated PBMC suspension and analyzed as a control in this experiment. Prior to the assays, the stimulated sample and unstimulated sample were diluted 2×, 8×, 32×, and 128× times to vary the analyte concentrations in the measurements, so that some of the assays may produce MC intensity values within the range of the standard curves. The median ^{197}Au signal intensities of AuNP attached to the classifier beads in these assays are presented in Figure 5. Substantially higher ^{197}Au signals were detected from the IL-4, IFNγ, and TNFα-classifier beads in the assays of the stimulated samples at all dilutions than from the unstimulated samples. This result indicates that we can detect the elevated secretion of cytokines and is in general agreement with the findings reported by Ai et al.[34] that PMA/ionomycin stimulation can trigger the release of a series of cytokines, including IL-4, IFNγ, and TNFα.

We employed the same assay conditions to measure a series of standard solutions containing nine target cytokines with known concentrations. A series of standard curves were then developed by fitting the assay results of standard solutions with four-parameter logistic regression (4P-LR) models (see Figure S5 in the Supporting Information). Using these standard curves, we tried to assess the concentrations of these cytokines in the unstimulated and stimulated samples. However, some assay results in Figure 5 are lower than the minimum values of the standard curves presented in Figure S5. Therefore, no concentration can be concluded from these low values. As a future work, more accurate reading may be obtained by improving the assay conditions to reduce the background signals at low analyte concentrations. Figure S6 in the Supporting Information summarizes our preliminary findings of the cytokine concentrations by fitting the assay results presented in Figure 5 into the standard curves shown in Figure S5. Since the dilution factors were taken into account in the calculation of the cytokine concentrations presented in Figure S6, ideally, we expect similar concentration values for the same sample measured from different dilutions. For the measurement of IL-4 concentration in the stimulated sample, 1×, 2×, 8×, 32×, 128× diluted samples reported IL-4 concentrations of a similar level in the stimulated sample, while for the unstimulated sample, none of the assays were able to produce enough signal intensities to assess the IL-4 concentrations, likely due to the low IL-4 concentration in the unstimulated sample. For the measurement of IFNγ concentration in the stimulated sample, the assays at different dilutions all reported very high signal intensities, which were higher than that of the most concentrated standard solution. Therefore, the IFNγ concentration in the stimulated sample assessed in this study is likely unreliable. The reason for the high IL-6 levels detected in the unstimulated PBMC samples is unclear. This study serves as a proof-of-concept experiment to demonstrate the potential of multiplex bead-based assays using MC. However, more studies are required to further optimize and eventually validate these bead-based assays for cytokine quantification.

CONCLUSIONS

In this study, we synthesized a set of 11 types of lanthanide-encoded microbeads by two-stage DisP. The metal content of the six metals in these microbeads was finely controlled by varying the feed of the metal complexes in the second stage of the DisP to produce microbeads generating signals in MC with median intensities of *ca.* 1000 counts per bead. These microbeads are uniform in size ($CV_{diameter}$ < 2%) and in metal content (RCV < 15%), which makes them good candidates of classifier beads in bead-based assays.

In this first report of a multiplex bead-based assay by MC, we examined a proof-of-concept experiment, targeting at cytokine analysis. To develop multiplexed bead-based sandwich immunoassays of cytokines and chemokines in MC, the surface of metal-encoded microbeads was modified with different types of Abs and employed as classifier beads to capture target analytes. To develop the reporter system and optimize assay conditions, a series of bead-based assays were first carried out to analyze a series of standard solutions containing up to nine types of cytokines and chemokines with known analyte concentrations. In the preliminary experiments, the MC signal intensities of reporter NPs were responsive to the concentration differences in the standard solutions. These assays showed high sensitivity at low analyte concentrations. However, non-specific binding of some of the detection Abs led to increased background noise issues. Background noise will compromise the detection limits of these assays. As a proof-of-concept experiment, the supernatants of two PBMC samples were analyzed by the nine-plex assays developed in this study for cytokines and chemokines. The assay results indicate that the supernatant of the PMA/ionomycin-stimulated sample contained elevated levels of IL-4, IFNγ, and TNFα, compared with that of the unstimulated sample. The results presented in this study show very promising progress on the development of bead-based sandwich immunoassays in MC.

https://doi.org/10.1021/acsmeasuresciau.2c00038
ACS Meas. Sci. Au 2022, 2, 629−640

■ ASSOCIATED CONTENT

Supporting Information

The Supporting Information is available free of charge at https://pubs.acs.org/doi/10.1021/acsmeasuresciau.2c00038.

Additional experimental details and results and discussion including SEM image of microbeads, background noise, and standard curves for bead-based assays (PDF)

■ AUTHOR INFORMATION

Corresponding Authors

Bedilu Allo − *Fluidigm Canada (now Standard BioTools Canada), Markham, Ontario L3R 4G5, Canada*; Email: bedilu.allo@fluidigm.com

Mitchell A. Winnik − *Department of Chemical Engineering and Applied Chemistry, University of Toronto, Toronto, Ontario M5S 3E5, Canada; Department of Chemistry, University of Toronto, Toronto, Ontario M5S 3H6, Canada;* orcid.org/0000-0002-2673-2141; Email: m.winnik@utoronto.ca

Author

Jieyi Liu − *Department of Chemical Engineering and Applied Chemistry, University of Toronto, Toronto, Ontario M5S 3E5, Canada*

Complete contact information is available at: https://pubs.acs.org/10.1021/acsmeasuresciau.2c00038

Author Contributions

CRediT: **Jieyi Liu** conceptualization (equal), data curation (equal), formal analysis (equal), writing-original draft (equal); **Bedilu Allo** conceptualization (equal), methodology (equal), writing-review & editing (equal).

Notes

The authors declare the following competing financial interest(s): Dr. Allo was an employee of Fluidigm Canada (now Standard BioTools Canada). He has since left the company.

Note: Fluidigm, Standard BioTools, CyTOF, EQ, MaxPar, and Helios are trademarks and/or registered trademarks of Standard BioTools Inc. or its affiliates in the United States and/or other countries. For Research Use Only. Not for use in diagnostic procedures.

■ ACKNOWLEDGMENTS

The Toronto authors thank Fluidigm Canada (now Standard BioTools Canada) and NSERC Canada (Alliance Project) for their support of this research. We thank Dr. Yefeng Zhang, Edmond Wong, Wilson Chung, Dr. Yang Liu, Taunia Closson, and Dr. Daniel Majonis for helpful discussions and assistance with the MC experiments.

■ REFERENCES

(1) Ramesh, G.; MacLean, A. G.; Philipp, M. T. Cytokines and Chemokines at the Crossroads of Neuroinflammation, Neurodegeneration, and Neuropathic Pain. *Mediactors Inflammation* **2013**, *2013*, 480739.

(2) Chatenoud, L.; Ferran, C.; Bach, J.-F. The Anti-CD3-Induced Syndrome: A Consequence of Massive In Vivo Cell Activation. In *Superantigens*; Fleischer, B., Sjögren, H. O., Eds.; Current Topics in Microbiology and Immunology; Springer: Berlin, Heidelberg, 1991; pp 121−134.

(3) Morgan, R. A.; Yang, J. C.; Kitano, M.; Dudley, M. E.; Laurencot, C. M.; Rosenberg, S. A. Case Report of a Serious Adverse Event Following the Administration of T Cells Transduced With a Chimeric Antigen Receptor Recognizing ERBB2. *Mol. Ther.* **2010**, *18*, 843−851.

(4) Finco, D.; Grimaldi, C.; Fort, M.; Walker, M.; Kiessling, A.; Wolf, B.; Salcedo, T.; Faggioni, R.; Schneider, A.; Ibraghimov, A.; Scesney, S.; Serna, D.; Prell, R.; Stebbings, R.; Narayanan, P. K. Cytokine Release Assays: Current Practices and Future Directions. *Cytokine* **2014**, *66*, 143−155.

(5) Vessillier, S.; Eastwood, D.; Fox, B.; Sathish, J.; Sethu, S.; Dougall, T.; Thorpe, S. J.; Thorpe, R.; Stebbings, R. Cytokine release assays for the prediction of therapeutic mAb safety in first-in man trials - Whole blood cytokine release assays are poorly predictive for TGN1412 cytokine storm. *J. Immunol. Methods* **2015**, *424*, 43−52.

(6) Fajgenbaum, D. C.; June, C. H. Cytokine Storm. *N. Engl. J. Med.* **2020**, *383*, 2255−2273.

(7) Diorio, C.; Shaw, P. A.; Pequignot, E.; Orlenko, A.; Chen, F.; Aplenc, R.; Barrett, D. M.; Bassiri, H.; Behrens, E.; DiNofia, A. M.; Gonzalez, V.; Koterba, N.; Levine, B. L.; Maude, S. L.; Meyer, N. J.; Moore, J. H.; Paessler, M.; Porter, D. L.; Bush, J. L.; Siegel, D. L.; Davis, M. M.; Zhang, D.; June, C. H.; Grupp, S. A.; Melenhorst, J. J.; Lacey, S. F.; Weiss, S. L.; Teachey, D. T. Diagnostic Biomarkers to Differentiate Sepsis from Cytokine Release Syndrome in Critically Ill Children. *Blood Adv.* **2020**, *4*, 5174−5183.

(8) Chen, G.; Wu, D.; Guo, W.; Cao, Y.; Huang, D.; Wang, H.; Wang, T.; Zhang, X.; Chen, H.; Yu, H.; Zhang, X.; Zhang, M.; Wu, S.; Song, J.; Chen, T.; Han, M.; Li, S.; Luo, X.; Zhao, J.; Ning, Q. Clinical and Immunological Features of Severe and Moderate Coronavirus Disease 2019. *J. Clin. Invest.* **2020**, *130*, 2620−2629.

(9) Huang, C.; Wang, Y.; Li, X.; Ren, L.; Zhao, J.; Hu, Y.; Zhang, L.; Fan, G.; Xu, J.; Gu, X.; Cheng, Z.; Yu, T.; Xia, J.; Wei, Y.; Wu, W.; Xie, X.; Yin, W.; Li, H.; Liu, M.; Xiao, Y.; Gao, H.; Guo, L.; Xie, J.; Wang, G.; Jiang, R.; Gao, Z.; Jin, Q.; Wang, J.; Cao, B. Clinical Features of Patients Infected with 2019 Novel Coronavirus in Wuhan, China. *Lancet* **2020**, *395*, 497−506.

(10) Herold, T.; Jurinovic, V.; Arnreich, C.; Lipworth, B. J.; Hellmuth, J. C.; von Bergwelt-Baildon, M.; Klein, M.; Weinberger, T. Elevated Levels of IL-6 and CRP Predict the Need for Mechanical Ventilation in COVID-19. *J. Allergy Clin. Immunol.* **2020**, *146*, 128−136.e4.

(11) Tang, Y.; Liu, J.; Zhang, D.; Xu, Z.; Ji, J.; Wen, C. Cytokine Storm in COVID-19: The Current Evidence and Treatment Strategies. *Front. Immunol.* **2020**, *11*, 1708.

(12) Que, Y.; Hu, C.; Wan, K.; Hu, P.; Wang, R.; Luo, J.; Li, T.; Ping, R.; Hu, Q.; Sun, Y.; Wu, X.; Tu, L.; Du, Y.; Chang, C.; Xu, G. Cytokine Release Syndrome in COVID-19: A Major Mechanism of Morbidity and Mortality. *Int. Rev. Immunol.* **2022**, *41*, 217−230.

(13) Price, C. P.; Newman, D. J. *Principles and Practice of Immunoassay*; Palgrave Macmillan: London, England, 1991.

(14) Surenaud, M.; Manier, C.; Richert, L.; Thiébaut, R.; Levy, Y.; Hue, S.; Lacabaratz, C. Optimization and Evaluation of Luminex Performance with Supernatants of Antigen-Stimulated Peripheral Blood Mononuclear Cells. *BMC Immunol.* **2016**, *17*, 44.

(15) McHugh, T. M. Chapter 33 Flow Microsphere Immunoassay for the Quantitative and Simultaneous Detection of Multiple Soluble Analytes. *Methods Cell Biol.* **1994**, *42*, 575−595.

(16) Carson, R. T.; Vignali, D. A. A. Simultaneous Quantitation of 15 Cytokines Using a Multiplexed Flow Cytometric Assay. *J. Immunol. Methods* **1999**, *227*, 41−52.

(17) Vignali, D. A. A. Multiplexed Particle-Based Flow Cytometric Assays. *J. Immunol. Methods* **2000**, *243*, 243−255.

(18) Kellar, K. L.; Kalwar, R. R.; Dubois, K. A.; Crouse, D.; Chafin, W. D.; Kane, B.-E. Multiplexed Fluorescent Bead-Based Immunoassays for Quantitation of Human Cytokines in Serum and Culture Supernatants. *Cytometry* **2001**, *45*, 27−36.

(19) Nolan, J. P.; Sklar, L. A. Suspension Array Technology: Evolution of the Flat-Array Paradigm. *Trends Biotechnol.* **2002**, *20*, 9−12.
(20) Kellar, K. L.; Iannone, M. A. Multiplexed Microsphere-Based Flow Cytometric Assays. *Exp. Hematol.* **2002**, *30*, 1227−1237.
(21) Harris, G.; Chen, W. Profiling of Cytokine and Chemokine Responses Using Multiplex Bead Array Technology. In *Immunoproteomics: Methods and Protocols*; Fulton, K. M., Twine, S. M., Eds.; *Methods in Molecular Biology*; Springer: New York, NY, 2019; pp 79−94.
(22) Knight, V.; Long, T.; Meng, Q. H.; Linden, M. A.; Rhoads, D. D. Variability in the Laboratory Measurement of Cytokines. *Arch. Pathol. Lab. Med.* **2020**, *144*, 1230−1233.
(23) Bandura, D. R.; Baranov, V. I.; Ornatsky, O. I.; Antonov, A.; Kinach, R.; Lou, X.; Pavlov, S.; Vorobiev, S.; Dick, J. E.; Tanner, S. D. Mass Cytometry: Technique for Real Time Single Cell Multitarget Immunoassay Based on Inductively Coupled Plasma Time-of-Flight Mass Spectrometry. *Anal. Chem.* **2009**, *81*, 6813−6822.
(24) Bendall, S. C.; Nolan, G. P.; Roederer, M.; Chattopadhyay, P. K. A deep profiler's guide to cytometry. *Trends Immunol.* **2012**, *33*, 323−332.
(25) Spitzer, M. H.; Nolan, G. P. Mass Cytometry: Single Cells, Many Features. *Cell* **2016**, *165*, 780−791.
(26) O'Gorman, W. E.; Hsieh, E. W. Y.; Savig, E. S.; Gherardini, P. F.; Hernandez, J. D.; Hansmann, L.; Balboni, I. M.; Utz, P. J.; Bendall, S. C.; Fantl, W. J.; Lewis, D. B.; Nolan, G. P.; Davis, M. M. Single-Cell Systems-Level Analysis of Human Toll-like Receptor Activation Defines a Chemokine Signature in Patients with Systemic Lupus Erythematosus. *J. Allergy Clin. Immunol.* **2015**, *136*, 1326−1336.
(27) Ajami, B.; Samusik, N.; Wieghofer, P.; Ho, P. P.; Crotti, A.; Bjornson, Z.; Prinz, M.; Fantl, W. J.; Nolan, G. P.; Steinman, L. Single-Cell Mass Cytometry Reveals Distinct Populations of Brain Myeloid Cells in Mouse Neuroinflammation and Neurodegeneration Models. *Nat. Neurosci.* **2018**, *21*, 541−551.
(28) Brown, H. M. G.; Kuhns, M. M.; Arriaga, E. A. High-Resolution Interrogation of Biological Systems via Mass Cytometry. *Proteomics for Biological Discovery*; John Wiley & Sons, Ltd, 2019; pp 215−246.
(29) Abdelrahman, A. I.; Dai, S.; Thickett, S. C.; Ornatsky, O.; Bandura, D.; Baranov, V.; Winnik, M. A. Lanthanide-Containing Polymer Microspheres by Multiple-Stage Dispersion Polymerization for Highly Multiplexed Bioassays. *J. Am. Chem. Soc.* **2009**, *131*, 15276−15283.
(30) Liu, J.; Wong, E. C. N.; Lu, E.; Jarzabek, J.; Majonis, D.; Winnik, M. A. Control of Metal Content in Polystyrene Microbeads Prepared with Metal Complexes of DTPA Derivatives. *Chem. Mater.* **2021**, *33*, 3802−3813.
(31) Guesdon, J. L.; Ternynck, T.; Avrameas, S. The Use of Avidin-Biotin Interaction in Immunoenzymatic Techniques. *J. Histochem. Cytochem.* **1979**, *27*, 1131−1139.
(32) Dudley, R. A.; Edwards, P.; Ekins, R. P.; Finney, D. J.; McKenzie, I. G.; Raab, G. M.; Rodbard, D.; Rodgers, R. P. Guidelines for Immunoassay Data Processing. *Clin. Chem.* **1985**, *31*, 1264−1271.
(33) Kenna, J. G.; Major, G. N.; Williams, R. S. Methods for Reducing Non-Specific Antibody Binding in Enzyme-Linked Immunosorbent Assays. *J. Immunol. Methods* **1985**, *85*, 409−419.
(34) Ai, W.; Li, H.; Song, N.; Li, L.; Chen, H. Optimal Method to Stimulate Cytokine Production and Its Use in Immunotoxicity Assessment. *Int. J. Environ. Res. Public Health* **2013**, *10*, 3834−3842.

https://doi.org/10.1021/acsmeasuresciau.2c00038
ACS Meas. Sci. Au 2022, 2, 629−640